THE JOURNAL OF PHYSICAL CHEMISTRY LETTERS
A JOURNAL OF THE AMERICAN CHEMICAL SOCIETY

pubs.acs.org/JPCL

Letter

Reconciling the Volcano Trend with the Butler–Volmer Model for the Hydrogen Evolution Reaction

Timothy T. Yang and Wissam A. Saidi*

Cite This: J. Phys. Chem. Lett. 2022, 13, 5310–5315

Read Online

ACCESS | Metrics & More | Article Recommendations | Supporting Information

ABSTRACT: The volcano trend has been widely utilized to forecast new optimum catalysts in computational chemistry while the Butler–Volmer relationship is the norm to explain current–potential characteristics from cyclic voltammetry in analytical chemistry. Herein, we develop an electrochemical model for hydrogen evolution reaction exchange currents that reconciles device-level chemistry, atomic-level volcano trend, and the Butler–Volmer relation. We show that the model is a function of the easy-to-compute hydrogen adsorption energy invariably obtained from first-principles atomic simulations. In addition, the model reproduces with high fidelity the experimental exchange currents for elemental metal catalysts over 15 orders of magnitude and is consistent with the recently proposed analytical model based on a data-driven approach. Our findings based on fundamental electrochemistry principles are general and can be applied to other reactions including CO_2 reduction, metal oxidation, and lithium (de)intercalation reactions.

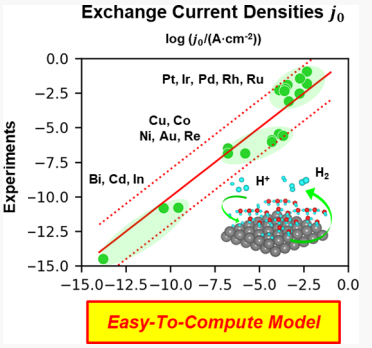

The hydrogen evolution reaction (HER) is a critical reaction for hydrogen production using renewable water-splitting methods. Currently, the grand HER challenge is in finding low-cost and highly efficient catalysts to replace or reduce the use of precious platinum, the most efficient HER catalyst. Computational screening using first-principles quantum-mechanical approaches has been instrumental not only for identifying the HER mechanism[1−6] at atomic scale but also in material's catalytic efficiency.[7−13] Central to the computational design approach is having a predictive, accurate, and easy-to-compute model to quantify the electrochemical catalytic efficiency of new candidate materials.

Following Sabatier's principle that the maximum reaction rate corresponds to the optimum reaction activity, Nørskov et al. proposed a computational model based on hydrogen adsorption free energy ΔG_H to determine HER exchange currents.[14] The Nørskov model explained the volcano trend—the optimum catalyst has a moderate adsorption strength indicated by $\Delta G_H = 0$ while the exchange currents decrease linearly with increasing or decreasing ΔG_H. Such a trend is obtained from a simple kinetic model assuming that ΔG_H is the only descriptor for exchange currents with other effects being universal for all metals. The computational framework based on ΔG_H has been widely employed for HER catalysts design because of the easy-to-compute descriptor, which can be obtained from first-principles quantum-mechanical methods.[3,4,15−23]

Despite the success of Nørskov's volcano trend, it has been the center of several debates. For instance, whether catalysts that bind hydrogen thermoneutrally are optimum catalysts for HER was challenged. By investigating the HER kinetic pathways on Pt (111), Peterson et al. argued that the sites that bind hydrogen atoms with $\Delta G_H > 0$ are HER-active while the $\Delta G_H \cong 0$ sites are not.[24] Investigating the same Pt (111) surface, Nørskov et al. showed that hydrogen atoms with $\Delta G_H \cong 0$ are HER-active[25] through hopping to the sites identified by Peterson et al.[24] with a negligible diffusion barrier. Schmickler et al. re-examined the Nørskov's volcano trend and showed that the calculated and experimental exchange current densities are off by 2 orders of magnitude for several metal surfaces.[26] This discrepancy is attributed to the growth of native oxide layers that cover the metal surfaces in an electrochemical environment, which are not accounted for in modeling.[26] In addition, this study argued that Nørskov's kinetic model is too simplistic and does not fully account for the electronic properties of the catalyst. In a recent study, we revisited Nørskov's model and showed that imposing a metal-dependent rate constant decreases the deviations from experimental results by up to 4 orders of magnitude.[27] Central to this finding was establishing a large reliable experimental database that was employed within a statistical approach to infer the dependence. Although the revised Nørskov model significantly improves the estimation on exchange currents, it is based on a data-driven approach that lacks a theoretical background. Furthermore, one of the concerns about the original or the revised Nørskov model is that it is not

Received: May 10, 2022
Accepted: June 2, 2022
Published: June 8, 2022

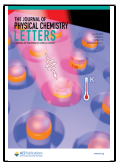

https://doi.org/10.1021/acs.jpclett.2c01411
J. Phys. Chem. Lett. 2022, 13, 5310−5315

reconcilable with the electrochemical modeling employed experimentally at the device level.

In analytical chemistry, HER has been widely evaluated by using cyclic voltammetry which provides current−potential characteristics (cyclic voltammogram) as an output of electrochemical behaviors. The norm to explain the cyclic voltammogram is the empirical Butler−Volmer relation $i \propto i_0 \exp[(\alpha_a F\eta/RT) - (\alpha_c F\eta/RT)]$ where $\alpha_{a/c}$ are the transfer coefficients for the anode/cathode reaction, F is the Faraday constant, T is the temperature, and η is the overpotential.[28,29] The exchange current i_0 is the most significant descriptor of HER rate with $\alpha_{a/c}$ the key indicator of the kinetics.[30] The Butler−Volmer relation is not only limited to HER[31−36] but also widely applied for many electrochemical reactions such as electron transfer reactions in modern lithium ion batteries[37−41] and fuel cells.[42−44]

Herein, we discuss theoretical insights based on the empirical volcano trend and propose an electrochemical model for HER exchange currents. First, we study the dependence of ΔG_H on the thermodynamics of HER pathways and show that the rate-determining step (rds) can be determined solely based on the value of ΔG_H. Such a dependency allows us to construct an electrochemical model for exchange currents based on the Butler−Volmer relation for a one-step, one-electron-transfer process. We show that the model is solely a function of ΔG_H and the transfer coefficient of the rds. The model is confirmed by performing atomic simulations using first-principles calculations employing 13 pure metals. In addition, we show that the model is equivalent to the revised Nørskov model for proton adsorption process that includes the material-dependent rate constant that was proposed in a previous study based on the statistical approach of experimental data.[27]

The overall hydrogen evolution reaction $H^+ + e^- \rightarrow \frac{1}{2}H_2$ proceeds with the Volmer−Heyrovsky or Volmer−Tafel pathways:

$$H^+ + e^- \leftrightarrow H^* \quad \text{(Volmer)}$$

$$H^* + e^- + H^+ \leftrightarrow H_2 \quad \text{(Heyrovsky)}$$

$$2H^* \leftrightarrow H_2 \quad \text{(Tafel)}$$

where H^+, H^*, and H_2 are the hydrogen atoms in the liquid, adsorbed, and gas state, respectively. The Gibbs free energies of the three elementary reactions are

$$\Delta g = \begin{cases} G_{H^*} - (G_{H^+} - |e|U) = \Delta G_H + |e|E & \text{(Volmer)} \\ G_{H_2} - (G_{H^*} + G_{H^+} - |e|U) = -\Delta G_H + |e|E & \text{(Heyrovsky)} \\ G_{H_2} - 2G_{H^*} = -2\Delta G_H & \text{(Tafel)} \end{cases} \tag{1}$$

where $E = U - U_{NHE}$ is the applied potential U in reference to the normal hydrogen electrode (NHE) U_{NHE}. To derive the final form in eq 1, we define $G_{H^+} = |e|U_{NHE} + \frac{1}{2}G_{H_2}$ as H^+ is in equilibrium with $H_2(g)$ at NHE, and use $\Delta G_H = G_{H^*} - \frac{1}{2}G_{H_2}$ as proposed by Nørskov et al.[14]

In the original literature, ΔG_H is defined as the free energy of the adsorbed state with respect to hydrogen gas under the standard conditions of 298 K and 1 atm, which is the free energy of the process $\frac{1}{2}H_2 \rightarrow H^*$.[14] However, this definition does not link the hydrogen adsorption from gas phase H_2 and from H^+ in acidic solution as stipulated for the overall HER. We posit that such a connection can be recovered from eq 1. For the Volmer reaction, at the equilibrium potential $E = 0$ where the exchange current density is defined, $\Delta g = \Delta G_H$ implies that the free energy changes from either the gas phase or the proton phase H^+ are identical. Additionally, for $E = 0$, the opposite signs of ΔG_H for the Volmer and the Heyrovsky (or Tafel) suggest that the two elementary steps in a reaction pathway cannot be both endothermic and exothermic at the same time. Therefore, on the basis of thermodynamics, we can posit that the Volmer reaction is the rds when $\Delta G_H > 0$ while the Heyrovsky is the rds for $\Delta G_H < 0$. In addition, the Tafel reaction can only be the rds at $\Delta G_H = 0$. We note that these thermodynamic-based conditions depend solely on ΔG_H while there are several kinetic factors that may alter the results in real electrochemical environments. These inferences are indeed justified by the HER kinetics determined from first-principles calculations.[45] In addition, the thermodynamic analysis implies that the maximum thermodynamic accessibility for any reaction pathways is at $\Delta G_H = 0$, which agrees with Nørskov's volcano trend.[14]

In general, the electrochemical current $j = e[C_f r_f - C_b r_b]$ is contributed by the forward and backward processes of a reaction, where e is the electron charge and $r_{f/b}$ and $C_{f/b}$ are the rate constant and the reactant concentration for the forward/backward reaction, respectively. $r_{f/b}$ can be expressed with the Butler−Volmer equation for a one-step, one-electron process as[46]

$$\begin{aligned} r_f &= k_0 \exp[-\alpha f(E - E^{0'})] \\ r_b &= k_0 \exp[(1-\alpha) f(E - E^{0'})] \end{aligned} \tag{2}$$

Here, α is the transfer coefficient and $f=F/RT$. E and $E^{0'}$ are the applied and the formal potentials associated with the rds. Note that $E^{0'}$ is the experimentally measured potential when $C_f = C_b$. The standard rate constant k_0 is defined as the value of the forward r_f or the backward r_b rate at $E^{0'}$; i.e., $k_0 = r_f = r_b$ at $E^{0'}$.[46] Using eq 2, we can express the total electrochemical current as

$$j = ek_0\{C_f \exp[-\alpha f(E - E^{0'})] - C_b \exp[(1-\alpha) f(E - E^{0'})]\} \tag{3}$$

Under the equilibrium condition $E = E_{eq}$ where E_{eq} is the equilibrium potential, the forward and backward currents have equal magnitudes that lead to a zero total current. This equality defines the exchange current density

$$\begin{aligned} j_0 &= ek_0 C_f \exp[-\alpha f(E_{eq} - E^{0'})] \\ &= ek_0 C_b \exp[(1-\alpha) f(E_{eq} - E^{0'})] \end{aligned} \tag{4}$$

Employing the Nernst relation, $\exp[f(E_{eq} - E_i^{0'})] = C_f/C_b$, we express the exchange current density of eq 4 as

$$j_0 = ek_0 C_f^{1-\alpha} C_b^{\alpha} \tag{5}$$

which is general for any single-step, single-electron-transfer process[46] and thus can be readily applied to the Volmer and Heyrovsky reactions. In addition, from the previous thermodynamic analysis of eq 1, we show that the total reaction rate depends on the rds for all cases except for the surface with $\Delta G_H = 0$. On the basis of these conditions, we will utilize eq 5 for HER in an acidic environment hereafter.

https://doi.org/10.1021/acs.jpclett.2c01411
J. Phys. Chem. Lett. 2022, 13, 5310−5315

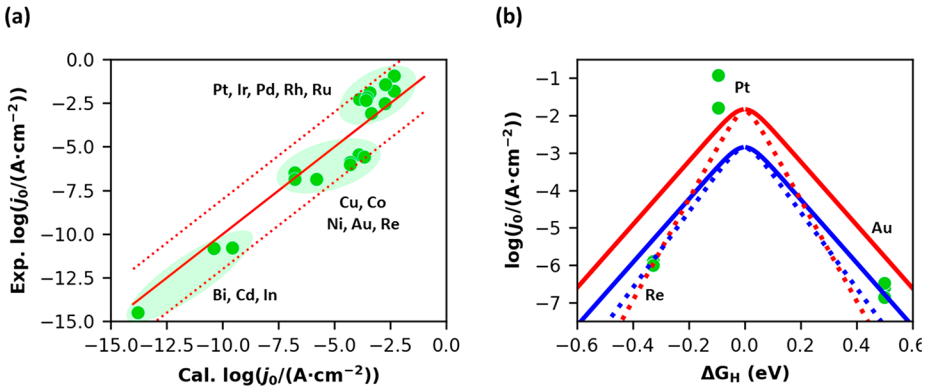

Figure 1. (a) Comparison between experimental and calculated j_0 of metal surfaces. The j_0 values are provided in the Supporting Information. (b) Volcano curves computed via eq 8. The red and blue lines are specified with C_{tot} for Pt and Au (or Re). The red (blue) solid and dashed lines are computed with α = 0.5 (0.5) and 0.8 (0.6), respectively. The filled green circles show experimental values of Re, Pt, and Au.

For a water−solid interface that is free from the diffusion limit of H^+ and H_2, only the proton concentration C_{H^+} near the adsorption sites and the concentration of adsorbed hydrogen atoms C_{H^*} control the HER process. Therefore, we can approximate the areal concentration of the total adsorption sites as $C_{tot} = C_{H^+} + C_{H^*}$.[46] For the Volmer reaction, $C_f = C_{H^+} = C_{tot}(1-\theta)$ and $C_b = C_{H^*} = C_{tot}\theta$, where θ is the fraction of occupied sites. For the Heyrovsky reaction, $C_f = C_{H^*} = C_{tot}\theta$ and $C_b = C_{tot}(1-\theta)$ as the forward reaction is controlled by the concentration of the adsorbed hydrogen atoms for proton reduction process and the backward reaction is controlled by the concentration of hydrogen gas near the empty adsorption sites. In summary, we cast the HER electrochemical exchange current model as

$$j_0 = \begin{cases} ek_0C_{tot}(1-\theta)^{(1-\alpha)}\theta^{\alpha} & \text{(Volmer)} \\ ek_0C_{tot}\theta^{(1-\alpha)}(1-\theta)^{\alpha} & \text{(Heyrovsky)} \end{cases} \quad (6)$$

We note that the Tafel reaction is not a charge-transfer reaction and hence cannot be described by the Butler−Volmer relation. The electrochemical model of eq 6 is general for HER with a distinct rds in an acidic environment. In addition, eq 6 is the central equation in our study that follows from fundamental electrochemistry principles in addition to the Butler−Volmer relation for a one-step, one-electron process. Considering that a proton reduction process begins with the Volmer reaction, this suggests rewriting eq 6 with H^+ concentration $C_{tot}(1-\theta)$ shown explicitly as

$$j_0 = \begin{cases} ek_0C_{tot}(1-\theta)(1-\theta)^{-\alpha}\theta^{\alpha} & \text{(Volmer)} \\ ek_0C_{tot}(1-\theta)\theta^{(1-\alpha)}(1-\theta)^{(\alpha-1)} & \text{(Heyrovsky)} \end{cases} \quad (7)$$

To validate the new model of eq 7 and cast into a computationally tractable model, we apply the model to thirteen transition metal surfaces. First, we obtained the hydrogen adsorption isotherms from ab initio thermodynamics (see the Supporting Information) and compared to three isotherm models: the Langmuir,[47−49] Frumkin,[49,50] and Temkin.[47,5152] Our analyses show that the Langmuir and Frumkin models agree well with the DFT results with a fitting confidence r^2 values over 0.87 and 0.94, respectively. In the rest of the study, we apply eq 7 based on the Langmuir model for simplicity as this form is amenable to an analytical solution. In addition, as we will show below, the Langmuir model allows us to gain more insight into the new electrochemical model and to compare with previous models.

Using the Langmuir model $\theta = K/(1+K)$ as well as defining the equilibrium constant as $K = \exp(-\Delta G_H/k_BT)$, we can rewrite $(1-\theta)^{-\alpha}\theta^{\alpha}$ and $\theta^{(1-\alpha)}(1-\theta)^{(\alpha-1)}$ in eq 7 to obtain,

$$j_0 = \begin{cases} ek_0C_{tot}(1-\theta)\exp(-\alpha\Delta G_H/k_BT) & \text{(Volmer)} \\ ek_0C_{tot}(1-\theta)\exp(-(1-\alpha)\Delta G_H/k_BT) & \text{(Heyrovsky)} \end{cases} \quad (8)$$

We note that $C_{tot}(1-\theta)$ can also be expressed as a function of ΔG_H using the Langmuir model. However, we explicitly include it here to show that the revised Nørskov model with the metal-dependent rate constant[27] follows naturally from the new model.

To fully define the new electrochemical model of eq 8, the rate constant k_0 must be determined. We hypothesize that k_0 is metal-independent on the basis of its original definition in eq 2. To obtain the universal k_0 value, we fit the theoretical model to experimental data. Specifically, we utilize j_0 and α from an experimental database that we previously compiled, which includes reports that minimized or otherwise accounted for the impacts of electrolyte/surface contamination, electrode roughness, and mass transfer effects[27] (also included in the Supporting Information). In addition, we use first-principles methods to compute the adsorption energy ΔG_H. Figure 1a shows the strong linear correlation between the experimental and computed j_0 currents as demonstrated with a r^2 value of 0.89. As seen from the figure, differences between the experimental and calculated j_0 for the 13 metals are within 2 orders of magnitude, as indicated by the dashed lines. These results, and particularly the significant correlations between computed and experimental j_0, lend strong credibility to the new model and the universality of k_0. Also, from the fit, we obtain $k_0 = 126\ s^{-1}$, which can be expressed as $k_0 = \frac{k_bT}{h}\exp\left(-\frac{0.65}{k_bT}\right)$, as will be reasoned and justified later.

Figure 1b shows the exchange current densities computed by using eq 8 with the fitted value of k_0. The blue and the red curves are computed by using C_{tot} for Au (or Re) and Pt, respectively, and are in agreement with their experimental values, as shown by green dots.[32,33,53−56] Here we use Pt as a reference given it is the most efficient single metal HER catalyst and chose Au and Re because these two metals have similar C_{tot}, except that Re has $\Delta G_H > 0$ and Au has $\Delta G_H < 0$.

https://doi.org/10.1021/acs.jpclett.2c01411
J. Phys. Chem. Lett. 2022, 13, 5310−5315

As seen from the figure, j_0 for high catalytic metals ($\Delta G_H \cong 0$) is less sensitive to α than j_0 for inert surfaces ($|\Delta G_H| > 0$). For example, for Pt with $\Delta G_H = -0.09$ eV, the calculated j_0 changes by less than a 1/2 order of magnitude between $\alpha = 0.5$ and 0.8. In contrast, for Au with $\Delta G_H = 0.50$ eV, the calculated j_0 differs by more than 1 order magnitude when α is off by 0.1. The sensitivity of the results to the combination between α and ΔG_H is justified given that the current depends exponentially on these terms, as seen in eq 8.

Having fully defined and established the new electrochemical model on the basis of first-principles methods and experimental results, we show next that this model is in agreement with the revised Nørskov model that accounts for the metal-dependent rate constant.[27] To demonstrate this clearly, it is convenient to introduce a new rate constant, k_0^{ana}:

$$\ln(k_0^{ana}) = \begin{cases} (1-\alpha)\dfrac{\Delta G_H}{k_B T} + \ln(k_0) & \text{(Volmer)} \\ -(1-\alpha)\dfrac{\Delta G_H}{k_B T} + \ln(k_0) & \text{(Heyrovsky)} \end{cases} \tag{9}$$

This new expression is the summation of the barrier of the backward reaction $(1-\alpha)\frac{\Delta G_H}{k_B T}$ and the metal-independent barrier $\ln(k_0)$. The introduction of k_0^{ana} is motivated given that Nørskov's model accounts only for the forward proton reduction process where the adsorption rate is explicitly shown as $\exp(-\Delta G_H/k_B T)$.[14] Thus, $\ln(k_0^{ana})$ encompasses all effects except for the forward adsorption rate. Substituting k_0 in eq 8 with the relations of eq 9, we obtain

$$j_0 = \begin{cases} e k_0^{ana} C_{tot}(1-\theta)\exp(-\Delta G_H/k_B T) & \text{(Volmer)} \\ e k_0^{ana} C_{tot}(1-\theta) & \text{(Heyrovsky)} \end{cases} \tag{10}$$

Equation 10 is similar to Nørskov's model with two important differences. First, in the original Nørskov's model, j_0 is driven by the proton adsorption through either an endothermic ($\Delta G_H > 0$) or exothermic ($\Delta G_H < 0$) process, with the Volmer or Heyrovsky reaction as the rds in eq 10, respectively. This distinction between the two pathways is consistent with the thermodynamic analysis discussion of eq 1 and with the computed kinetic barriers on metal surfaces.[26]

Second, different from the Nørskov's assumption that stipulates the universality of $k_0^{ana} = 200$ s^{-1} site^{-1} for all metal surfaces, we previously uncovered its material dependence based on a data-driven statistical approach of experimental measurements.[27] Namely, we find that k_0^{ana} has the empirical form[27]

$$\ln(k_0^{ana}) = \begin{cases} 23.16\Delta G_H + 3.17 & \text{(Volmer)} \\ -23.16\Delta G_H + 3.17 & \text{(Heyrovsky)} \end{cases} \tag{11}$$

and is indeed consistent with the definition of eq 9. For each of the rds, by separately equating the first or the second term of eqs 9 and 11, we obtain $(1-\alpha)\frac{\Delta G_H}{k_B T} = 23.16\Delta G_H$ which implies $\alpha = 0.4$ and $\ln(k_0) = 3.17$. The value obtained for $\alpha = 0.4$ is close to 0.5, which is recommended experimentally.[32,33,46] On the other hand, expressing k_0 in terms of the transition state theory $k_0 = \frac{k_b T}{h}\exp\left(-\frac{\Delta G^+}{k_b T}\right)$, we obtain an activation energy $\Delta G^+ = 0.7$ eV, which is close to the Tafel activation energy 0.8 eV on 12 pure metal surfaces.[25,45] Note that a detailed comparison between the experimental values of j_0, the values computed by using our electrochemical model of eq 8 with the relation of eq 11, and the Nørskov's model is discussed in the Supporting Information and ref 27.

In summary, this Letter reconciles the volcano trend and the Butler–Volmer relationship. The first is widely employed in computational modeling to design new catalysts based on an easy-to-compute descriptor while the second is the norm in analytical chemistry to interpret cyclic voltammograms. In addition, we derive a new electrochemical model based on the Butler–Volmer relation of a one-step, one-electron-transfer process in conjunction with ΔG_H, which is easy to compute as it depends only on ΔG_H and the transfer coefficient of the rate-determining step. We validate the model by comparing to a large set of experimental database for metal surfaces that have been verified before. Finally, we show that the model agrees with the Nørskov model after accounting for the metals' dependence in the rate constant, which has been uncovered recently based on a data-driven approach.

The framework of constructing the new electrochemical model not only is limited to HER but also is general for other electrochemical reactions that follow the Butler–Volmer relation such as CO_2 reduction,[57] metal oxidation,[58] and lithium (de)intercalation reactions.[57,59] This is also justified because the Langmuir,[47−49] Frumkin,[49,50] and Temkin[47,51] models can be generally applied to adsorption isotherms. Thus, through a systematic study of the empirical relation between the computational adsorption free energy and the experimental exchange currents, general values of α and k_0 can be found for a reaction with similar electrochemical conditions.

Methods. The first-principles density functional theory (DFT) calculations are performed by using the Vienna Ab Initio Simulation Package (VASP) with projector augmented wave (PAW) potentials to describe electron–nucleus interactions.[60−63] The Kohn–Sham equations with periodic boundary conditions are resolved by using the revised Perdew–Burke–Ernzerhof[64] in conjunction with van der Waals (vdW) correction based Tkatchenko–Scheffler scheme.[65,66] For all metals except Co, we have confirmed that spin polarization effects are negligible. See the Supporting Information for further details.

■ ASSOCIATED CONTENT

Supporting Information

The Supporting Information is available free of charge at https://pubs.acs.org/doi/10.1021/acs.jpclett.2c01411.

Computational details, adsorption isotherms based on Langmuir and Frumkin, and comparison between the Nørskov model and the new electrochemical model (PDF)

■ AUTHOR INFORMATION

Corresponding Author

Wissam A. Saidi − *Department of Materials Science and Engineering, University of Pittsburgh, Pittsburgh, Pennsylvania 15260, United States;* orcid.org/0000-0001-6714-4832; Email: alsaidi@pitt.edu

https://doi.org/10.1021/acs.jpclett.2c01411
J. Phys. Chem. Lett. 2022, 13, 5310−5315

Author

Timothy T. Yang − *Department of Materials Science and Engineering, University of Pittsburgh, Pittsburgh, Pennsylvania 15260, United States;* orcid.org/0000-0002-5785-0511

Complete contact information is available at: https://pubs.acs.org/10.1021/acs.jpclett.2c01411

Notes

The authors declare no competing financial interest.

■ ACKNOWLEDGMENTS

W.A.S. and T.T.Y. acknowledge financial support from the National Science Foundation (Award CBET-2130804). We are grateful for computing time provided in part by the CRC resources at the University of Pittsburgh and Argonne Leadership Computing Facility, which is a DOE Office of Science User Facility supported under Contract DE-AC02-06CH11357.

■ REFERENCES

(1) Li, J.; Stenlid, J. H.; Ludwig, T.; Lamoureux, P. S.; Abild-Pedersen, F. Modeling Potential-Dependent Electrochemical Activation Barriers: Revisiting the Alkaline Hydrogen Evolution Reaction. *J. Am. Chem. Soc.* **2021**, *143* (46), 19341−19355.

(2) Kronberg, R.; Lappalainen, H.; Laasonen, K. Revisiting the Volmer−Heyrovský Mechanism of Hydrogen Evolution on a Nitrogen Doped Carbon Nanotube: Constrained Molecular Dynamics Versus the Nudged Elastic Band Method. *Phys. Chem. Chem. Phys.* **2020**, *22* (19), 10536−10549.

(3) Yang, T. T.; Tan, T. L.; Saidi, W. A. High Activity toward the Hydrogen Evolution Reaction on the Edges of Mos2-Supported Platinum Nanoclusters Using Cluster Expansion and Electrochemical Modeling. *Chem. Mater.* **2020**, *32* (3), 1315−1321.

(4) Yang, T. T.; Saidi, W. A. Graphene Activation Explains the Enhanced Hydrogen Evolution on Graphene-Coated Molybdenum Carbide Electrocatalysts. *J. Phys. Chem. Lett.* **2020**, *11* (7), 2759−2764.

(5) Liu, X.; Li, B.; Soto, F. A.; Li, X.; Unocic, R. R.; Balbuena, P. B.; Harutyunyan, A. R.; Hone, J.; Esposito, D. V. Enhancing Hydrogen Evolution Activity of Monolayer Molybdenum Disulfide Via a Molecular Proton Mediator. *ACS Catal.* **2021**, *11* (19), 12159−12169.

(6) Sun, T.; Zang, W.; Yan, H.; Li, J.; Zhang, Z.; Bu, Y.; Chen, W.; Wang, J.; Lu, J.; Su, C. Engineering the Coordination Environment of Single Cobalt Atoms for Efficient Oxygen Reduction and Hydrogen Evolution Reactions. *ACS Catal.* **2021**, *11* (8), 4498−4509.

(7) Ding, J.; Ji, Y.; Li, Y.; Hong, G. Monoatomic Platinum-Embedded Hexagonal Close-Packed Nickel Anisotropic Superstructures as Highly Efficient Hydrogen Evolution Catalyst. *Nano Lett.* **2021**, *21* (22), 9381−9387.

(8) Zhang, J.; Wang, E.; Cui, S.; Yang, S.; Zou, X.; Gong, Y. Single-Atom Pt Anchored on Oxygen Vacancy of Monolayer Ti3c2tx for Superior Hydrogen Evolution. *Nano Lett.* **2022**, *22* (3), 1398−1405.

(9) Jia, Y.; Huang, T.-H.; Lin, S.; Guo, L.; Yu, Y.-M.; Wang, J.-H.; Wang, K.-W.; Dai, S. Stable Pd−Cu Hydride Catalyst for Efficient Hydrogen Evolution. *Nano Lett.* **2022**, *22* (3), 1391−1397.

(10) Zhao, G.; Xia, L.; Cui, P.; Qian, Y.; Jiang, Y.; Zhao, Y.; Pan, H.; Dou, S. X.; Sun, W. Atomic-Level Modulation of the Interface Chemistry of Platinum−Nickel Oxide toward Enhanced Hydrogen Electrocatalysis Kinetics. *Nano Lett.* **2021**, *21* (11), 4845−4852.

(11) Greeley, J.; Nørskov, J. K. Large-Scale, Density Functional Theory-Based Screening of Alloys for Hydrogen Evolution. *Surf. Sci.* **2007**, *601* (6), 1590−1598.

(12) Santos, E.; Lundin, A.; Pötting, K.; Quaino, P.; Schmickler, W. Model for the Electrocatalysis of Hydrogen Evolution. *Phys. Rev. B* **2009**, *79* (23), 235436.

(13) Yang, T. T.; Saidi, W. A. Tuning the Hydrogen Evolution Activity of B-Mo2c Nanoparticles Via Control of Their Growth Conditions. *Nanoscale* **2017**, *9* (9), 3252−3260.

(14) Nørskov, J. K.; Bligaard, T.; Logadottir, A.; Kitchin, J. R.; Chen, J. G.; Pandelov, S.; Stimming, U. Trends in the Exchange Current for Hydrogen Evolution. *J. Electrochem. Soc.* **2005**, *152* (3), J23.

(15) Xiao, Y.; Shen, C.; Long, T. Theoretical Establishment and Screening of an Efficient Catalyst for N2 Electroreduction on Two-Dimensional Transition-Metal Borides (Mbenes). *Chem. Mater.* **2021**, *33* (11), 4023−4034.

(16) Zhang, Y.-J.; Sethuraman, V.; Michalsky, R.; Peterson, A. A. Competition between Co2 Reduction and H2 Evolution on Transition-Metal Electrocatalysts. *ACS Catal.* **2014**, *4* (10), 3742−3748.

(17) Gauthier, J. A.; King, L. A.; Stults, F. T.; Flores, R. A.; Kibsgaard, J.; Regmi, Y. N.; Chan, K.; Jaramillo, T. F. Transition Metal Arsenide Catalysts for the Hydrogen Evolution Reaction. *J. Phys. Chem. C* **2019**, *123* (39), 24007−24012.

(18) Abghoui, Y.; Skúlason, E. Hydrogen Evolution Reaction Catalyzed by Transition-Metal Nitrides. *J. Phys. Chem. C* **2017**, *121* (43), 24036−24045.

(19) Tang, Q.; Jiang, D.-e. Mechanism of Hydrogen Evolution Reaction on 1t-Mos2 from First Principles. *ACS Catal.* **2016**, *6* (8), 4953−4961.

(20) Di Liberto, G.; Cipriano, L. A.; Pacchioni, G. Role of Dihydride and Dihydrogen Complexes in Hydrogen Evolution Reaction on Single-Atom Catalysts. *J. Am. Chem. Soc.* **2021**, *143* (48), 20431−20441.

(21) Feng, G.; Ning, F.; Song, J.; Shang, H.; Zhang, K.; Ding, Z.; Gao, P.; Chu, W.; Xia, D. Sub-2 Nm Ultrasmall High-Entropy Alloy Nanoparticles for Extremely Superior Electrocatalytic Hydrogen Evolution. *J. Am. Chem. Soc.* **2021**, *143* (41), 17117−17127.

(22) Li, Y.; Li, S.; Nagarajan, A. V.; Liu, Z.; Nevins, S.; Song, Y.; Mpourmpakis, G.; Jin, R. Hydrogen Evolution Electrocatalyst Design: Turning Inert Gold into Active Catalyst by Atomically Precise Nanochemistry. *J. Am. Chem. Soc.* **2021**, *143* (29), 11102−11108.

(23) Gu, G. H.; Lim, J.; Wan, C.; Cheng, T.; Pu, H.; Kim, S.; Noh, J.; Choi, C.; Kim, J.; Goddard, W. A.; Duan, X.; Jung, Y. Autobifunctional Mechanism of Jagged Pt Nanowires for Hydrogen Evolution Kinetics Via End-to-End Simulation. *J. Am. Chem. Soc.* **2021**, *143* (14), 5355−5363.

(24) Lindgren, P.; Kastlunger, G.; Peterson, A. A. A Challenge to the G ∼ 0 Interpretation of Hydrogen Evolution. *ACS Catal.* **2020**, *10* (1), 121−128.

(25) Skúlason, E.; Karlberg, G. S.; Rossmeisl, J.; Bligaard, T.; Greeley, J.; Jónsson, H.; Nørskov, J. K. Density Functional Theory Calculations for the Hydrogen Evolution Reaction in an Electrochemical Double Layer on the Pt(111) Electrode. *Phys. Chem. Chem. Phys.* **2007**, *9* (25), 3241−3250.

(26) Quaino, P.; Juarez, F.; Santos, E.; Schmickler, W. Volcano Plots in Hydrogen Electrocatalysis − Uses and Abuses. *Beilstein J. Nanotechnoo* **2014**, *5*, 846−854.

(27) Yang, T. T.; Patil, R. B.; McKone, J. R.; Saidi, W. A. Revisiting Trends in the Exchange Current for Hydrogen Evolution. *Catal. Sci. Technol.* **2021**, *11* (20), 6832−6838.

(28) Guidelli, R.; Compton, R. G.; Feliu, J. M.; Gileadi, E.; Lipkowski, J.; Schmickler, W.; Trasatti, S. Defining the Transfer Coefficient in Electrochemistry: An Assessment (Iupac Technical Report). *J. Pure and Applied Chemistry* **2014**, *86* (2), 245−258.

(29) Dickinson, E. J. F.; Wain, A. J. The Butler-Volmer Equation in Electrochemical Theory: Origins, Value, and Practical Application. *J. Electroanal. Chem.* **2020**, *872*, 114145.

(30) Shinagawa, T.; Garcia-Esparza, A. T.; Takanabe, K. Insight on Tafel Slopes from a Microkinetic Analysis of Aqueous Electrocatalysis for Energy Conversion. *Sci. Rep.* **2015**, *5* (1), 13801.

(31) Sheng, W.; Gasteiger, H. A.; Shao-Horn, Y. Hydrogen Oxidation and Evolution Reaction Kinetics on Platinum: Acid Vs Alkaline Electrolytes. *J. Electrochem. Soc.* **2010**, *157* (11), B1529.
(32) Zheng, J.; Sheng, W.; Zhuang, Z.; Xu, B.; Yan, Y. Universal Dependence of Hydrogen Oxidation and Evolution Reaction Activity of Platinum-Group Metals on Ph and Hydrogen Binding Energy. *Sci. Adv.* **2016**, *2* (3), No. e1501602.
(33) Durst, J.; Simon, C.; Hasché, F.; Gasteiger, H. A. Hydrogen Oxidation and Evolution Reaction Kinetics on Carbon Supported Pt, Ir, Rh, and Pd Electrocatalysts in Acidic Media. *J. Electrochem. Soc.* **2015**, *162* (1), F190−F203.
(34) Rheinländer, P. J.; Herranz, J.; Durst, J.; Gasteiger, H. A. Kinetics of the Hydrogen Oxidation/Evolution Reaction on Polycrystalline Platinum in Alkaline Electrolyte Reaction Order with Respect to Hydrogen Pressure. *J. Electrochem. Soc.* **2014**, *161* (14), F1448−F1457.
(35) Durst, J.; Siebel, A.; Simon, C.; Hasché, F.; Herranz, J.; Gasteiger, H. A. New Insights into the Electrochemical Hydrogen Oxidation and Evolution Reaction Mechanism. *Energy Environ. Sci.* **2014**, *7* (7), 2255−2260.
(36) Huang, Y.; Nielsen, R. J.; Goddard, W. A. Reaction Mechanism for the Hydrogen Evolution Reaction on the Basal Plane Sulfur Vacancy Site of Mos2 Using Grand Canonical Potential Kinetics. *J. Am. Chem. Soc.* **2018**, *140* (48), 16773−16782.
(37) Dreyer, W.; Guhlke, C.; Müller, R. A New Perspective on the Electron Transfer: Recovering the Butler−Volmer Equation in Non-Equilibrium Thermodynamics. *Phys. Chem. Chem. Phys.* **2016**, *18* (36), 24966−24983.
(38) Liu, S.; Jiang, J.; Shi, W.; Ma, Z.; Wang, L. Y.; Guo, H. Butler−Volmer-Equation-Based Electrical Model for High-Power Lithium Titanate Batteries Used in Electric Vehicles. *IEEE Transactions on Industrial Electronics* **2015**, *62* (12), 7557−7568.
(39) Fraggedakis, D.; McEldrew, M.; Smith, R. B.; Krishnan, Y.; Zhang, Y.; Bai, P.; Chueh, W. C.; Shao-Horn, Y.; Bazant, M. Z. Theory of Coupled Ion-Electron Transfer Kinetics. *Electrochim. Acta* **2021**, *367*, 137432.
(40) Allagui, A.; Benaoum, H.; Wang, C. Deformed Butler−Volmer Models for Convex Semilogarithmic Current-Overpotential Profiles of Li-Ion Batteries. *J. Phys. Chem. C* **2022**, *126* (6), 3029−3036.
(41) Azhagurajan, M.; Kajita, T.; Itoh, T.; Kim, Y.-G.; Itaya, K. In Situ Visualization of Lithium Ion Intercalation into Mos2 Single Crystals Using Differential Optical Microscopy with Atomic Layer Resolution. *J. Am. Chem. Soc.* **2016**, *138* (10), 3355−3361.
(42) Noren, D. A.; Hoffman, M. A. Clarifying the Butler−Volmer Equation and Related Approximations for Calculating Activation Losses in Solid Oxide Fuel Cell Models. *J. Power Sources* **2005**, *152*, 175−181.
(43) Vijay, P.; Tadé, M. O. Improved Approximation for the Butler-Volmer Equation in Fuel Cell Modelling. *Comput. Chem. Eng.* **2017**, *102*, 2−10.
(44) Li, Q.; Li, G. Modeling of the Solid Oxide Fuel Cell Anode Based on a New Analytical Model Using Nonlinear Butler-Volmer Expression. *Ionics* **2021**, *27* (7), 3063−3076.
(45) Tang, M. T.; Liu, X.; Ji, Y.; Norskov, J. K.; Chan, K. Modeling Hydrogen Evolution Reaction Kinetics through Explicit Water−Metal Interfaces. *J. Phys. Chem. C* **2020**, *124* (51), 28083−28092.
(46) Bard, A. J.; Faulkner, L. R. *Electrochemical Method: Fundamentals and Applications*; John Wiley & Sons, Inc.: 2010.
(47) Jiang, H.; Yang, Y.; Sun, S.; Yu, J. Adsorption of Lithium Ions on Lithium-Aluminum Hydroxides: Equilibrium and Kinetics. *Can. J. Chem. Eng.* **2020**, *98* (2), 544−555.
(48) Recepoğlu, Y. K.; Kabay, N.; Yılmaz-Ipek, İ.; Arda, M.; Yoshizuka, K.; Nishihama, S.; Yüksel, M. Equilibrium and Kinetic Studies on Lithium Adsorption from Geothermal Water by Λ-Mno2. *Solvent Extr. Ion Exch.* **2017**, *35* (3), 221−231.
(49) Zhong, J.; Lin, S.; Yu, J. Li+ Adsorption Performance and Mechanism Using Lithium/Aluminum Layered Double Hydroxides in Low Grade Brines. *Desalination* **2021**, *505*, 114983.
(50) Levi, M. D.; Aurbach, D. Frumkin Intercalation Isotherm — a Tool for the Description of Lithium Insertion into Host Materials: A Review. *Electrochim. Acta* **1999**, *45* (1), 167−185.
(51) Lane, J. M. D.; Leung, K.; Thompson, A. P.; Cuneo, M. E. Water Desorption from Rapidly-Heated Metal Oxide Surfaces—First Principles, Molecular Dynamics, and the Temkin Isotherm. *J. Condens. Matter Phys.* **2018**, *30* (46), 465002.
(52) Foo, K. Y.; Hameed, B. H. Insights into the Modeling of Adsorption Isotherm Systems. *Chem. Eng. J.* **2010**, *156* (1), 2−10.
(53) Perez, J.; Gonzalez, E. R.; Villullas, H. M. Hydrogen Evolution Reaction on Gold Single-Crystal Electrodes in Acid Solutions. *J. Phys. Chem. B* **1998**, *102* (52), 10931−10935.
(54) Štrbac, S.; Srejić, I.; Rakočević, Z. Electrocatalysis of Hydrogen Evolution Reaction on Au(111) by Spontaneously Deposited Iridium in Acid Solution. *J. Electrochem. Soc.* **2018**, *165* (15), J3335−J3341.
(55) Rivera, J. G.; Garcia-Garcia, R.; Coutino-Gonzalez, E.; Orozco, G. Hydrogen Evolution Reaction on Metallic Rhenium in Acid Media with or without Methanol. *Int. J. Hydrogen Energy* **2019**, *44* (50), 27472−27482.
(56) Garcia-Garcia, R.; Ortega-Zarzosa, G.; Rincón, M. E.; Orozco, G. The Hydrogen Evolution Reaction on Rhenium Metallic Electrodes: A Selected Review and New Experimental Evidence. *Electrocatalysis* **2015**, *6* (3), 263−273.
(57) Hossain, M. D.; Huang, Y.; Yu, T. H.; Goddard, W. A., III; Luo, Z. Reaction Mechanism and Kinetics for Co2 Reduction on Nickel Single Atom Catalysts from Quantum Mechanics. *Nat. Commun.* **2020**, *11* (1), 2256.
(58) van Ede, M. C.; Earls, C. J.; Fichtner, A.; Angst, U. Electrochemical Tomography as a Nondestructive Technique to Study Localized Corrosion of Metals. *npj Mater. Degrad.* **2021**, *5* (1), 58.
(59) Bai, P.; Bazant, M. Z. Charge Transfer Kinetics at the Solid−Solid Interface in Porous Electrodes. *Nat. Commun.* **2014**, *5* (1), 3585.
(60) Kresse, G.; Hafner, J. Ab Initio Molecular Dynamics for Liquid Metals. *Phys. Rev. B* **1993**, *47* (1), 558−561.
(61) Kresse, G.; Hafner, J. Ab Initio Molecular Dynamics for Open-Shell Transition Metals. *Phys. Rev. B* **1993**, *48* (17), 13115−13118.
(62) Kresse, G.; Hafner, J. Ab-Initio Molecular-Dynamics Simulation of the Liquid-Metal Amorphous-Semiconductor Transition in Germanium. *Phys. Rev. B* **1994**, *49* (20), 14251−14269.
(63) Kresse, G.; Joubert, D. From Ultrasoft Pseudopotentials to the Projector Augmented-Wave Method. *Phys. Rev. B* **1999**, *59* (3), 1758−1775.
(64) Hammer, B.; Hansen, L. B.; Nørskov, J. K. Improved Adsorption Energetics within Density-Functional Theory Using Revised Perdew-Burke-Ernzerhof Functionals. *Phys. Rev. B* **1999**, *59*, 7413.
(65) Tkatchenko, A.; Scheffler, M. Accurate Molecular Van Der Waals Interactions from Ground-State Electron Density and Free-Atom Reference Data. *Phys. Rev. Lett.* **2009**, *102* (7), 073005.
(66) Al-Saidi, W.; Voora, V. K.; Jordan, K. D. An Assessment of the Vdw-Ts Method for Extended Systems. *J. Chem. Theory Comput.* **2012**, *8* (4), 1503−1513.

https://doi.org/10.1021/acs.jpclett.2c01411
J. Phys. Chem. Lett. 2022, 13, 5310−5315